International Journal of Pharmaceutics 394 (2010) 106–114

Contents lists available at ScienceDirect

International Journal of Pharmaceutics

journal homepage: www.elsevier.com/locate/ijpharm

QSAR analysis of antitumor active amides and quinolones from thiophene series

B. Bertoša[a,*], M. Aleksić[b], G. Karminiski-Zamola[b], S. Tomić[a]

[a] Division of Physical Chemistry, Ruđer Bošković Institute, Bijenička cesta 54, 10 000 Zagreb, Croatia
[b] Faculty of Chemical Engineering and Technology, Marulićev trg 19, 10 000 Zagreb, Croatia

ARTICLE INFO

Article history:
Received 29 March 2010
Received in revised form 7 May 2010
Accepted 8 May 2010
Available online 21 May 2010

Keywords:
QSAR
VolSurf
Antitumor activity
Quinolones

ABSTRACT

QSAR models for predicting antitumor activity of heterocyclic amides and quinolones from benzo[*b*]thiophene-, thieno[3,2-*b*]thiophene- and thieno[2,3-*b*], thiophene series against MiaPaCa-2 and MCF-7 cells were built. Complete dataset consisted of 59 compounds and several QSAR models with different predictive ability were derived. Beside standard approaches for building QSAR models, the approach based on a small dataset of 10 compounds selected regarding the results of principal component analysis was tested. The latter approach was shown as successful and can be useful for planning future experiments in order to speed up and simplify the search for new drug candidates. Based on the derived QSAR models, the most important properties for compound's antitumor activity against MiaPaCa-2 and MCF-7 cells were identified. Volume, sum of the hydrophobic surfaces and presence of the group that can be easily ionized in the pH range from 4 to 9, were found to be highly important for successful antitumor activity of the examined heterocyclic amides and quinolones. New compounds, with potentially higher biological activity against MiaPaCa-2 and MCF-7 cells, were proposed. Their activities were predicted using the derived QSAR models and the proposed compounds were shown as promising antitumor candidates.

1. Introduction

There is a broad range of published data describing the synthesis and antitumor activity of heterocyclic condensed quinolones. For instance, derivatives of 7*H*-pyrido[1,2,3*de*] [1,4]benzothiazine-6-carboxylic acid exhibited significant inhibitory activity against mammalian topoisomerase II (Coughlin et al., 1995). The quinobenzoxazine compounds, derived from antibacterial quinolones, showed *in vitro* and *in vivo* activity against murine and human tumors. In this contribution, it was detected, that the relative DNA binding affinity of the quinobenzoxazine compounds correlates with their cytotoxicity, their ability to inhibit gyrase-DNA complex formation (Kwok et al., 1999). Pyranoquinoline-2-ones were synthesized and evaluated for their *in vitro* cytotoxicity against a panel of human tumor cell lines (Yang et al., 1999), while 2-arylquinazolinones displayed significant growth inhibitory action against tumor cell lines. Some of them were potent inhibitors of tubulin polymerization and displayed selective activity against P-gp-expressing epidermoid carcinoma of the nasopharynx (Xia et al., 2001). Indolo-, pyrrolo-, and benzofuro-quinolones, and anilinoindoloquinolone derivatives were synthesized and evaluated *in vitro* against a 3-cell line panel consisting of MCF7, NCI-H460, and SF268. The results have shown that cytotoxicity decreases in the order of anilinoindoloquinolones > indoloquinolones > pyrroloquinolones > benzofuroquinolone (Chen et al., 2002). It was discovered that a series of substituted 1,8-naphthyridine-3-carboxylic acids possessed moderate cytotoxic activity. The structure–activity relationship was investigated in this series of compounds by changing N-1 and C-7 positions and the core ring structure itself and evaluated the synthesized compounds against several murine and human tumor cells (Chilin et al., 2000). Methoxymethylfuro[2,3-*h*]quinolin-2(1*H*)-ones inhibited topoisomerase II, leading to a moderate antiproliferative activity in mammalian cells. The antiproliferative activity was also tested upon UVA irradiation in mammalian cells; all compounds showed higher activity than 8-MOP (8-methoxypsoralen-well known and most used furocoumarin for photoactivation and photochemotherapeutic tests), without mutagenicity and skin phototoxicity (Marzano et al., 2004).

In our earlier studies (Ćaleta et al., 2009; Ester et al., 2009; Jarak et al., 2006, 2005; Dogan Koružnjak et al., 2002, 2003) on the synthesis and antitumor evaluation of a number of benzo[*b*]thieno[2,3-*c*]quinolones with different substituents, we concluded that *N,N*-dimethylamino-propyl-9-methoxy, *N,N*-dimethylamino-propyl-9-methoxycarbonyl- and *N,N*-dimethylamino-propyl-9-*N*-pheny-amido substituted title compounds exhibited the most potent antitumor effect on examined human tumor cell lines. It seems that the substitution on the quinolone ring nitrogen with *N,N*-dimethylamino-propyl substituent was responsible for antitumor activity even when

* Corresponding author. Tel.: +385 1 456 10 25; fax: +385 1 468 02 45.
E-mail address: bbertosa@irb.hr (B. Bertoša).

0378-5173/$ – see front matter © 2010 Elsevier B.V. All rights reserved.
doi:10.1016/j.ijpharm.2010.05.014

the benzene ring in benzothiophene moiety was substituted with thiophene nuclei and in two compounds where amido group in the position 9 was substituted also with *N,N*-dimethylamino-propyl group. Isopropylamidino-substituted compounds from the same series substituted on position 2 or 9 showed very potent but very different antitumor activity. Compounds with isopropylamidino substituent in the position 2 and methoxycarbony subtituent in the position 9 and *vice versa* showed the most potent activity. The presented cell-cycle distribution related results strongly suggest that these compounds may act as topoisomerase "poisons". Studies on interactions of these compounds with ds-DNA and RNA have shown that they efficiently bind to double-strained polynucleotides by intercalation (Dogan Koružnjak et al., 2002, 2003). Since it is well known that intercalators act as topoisomerase inhibitors or "poisons" it is reasonable to propose the intercalation as main mode of action. Methoxycarbonyl groups may act as additionally "ankers" to DNA (Jarak et al., 2005). When the quinolone group in the condensed benzo[*b*]thiophene[2,3-*c*]quinolones was substituted with the naphthyridone group and amidino group with cyclic amidino group; imidazolinyl group in the 2-position the antitumor effect increased (Ester et al., 2009). When the benzene nuclei in benzothiophene assay are substituted with thiophene in thienothiophene part of the quinolones, antitumor activity decreased (Jarak et al., 2006).

Quantitative Structure–Activity Relationship (QSAR) studies have often been used to find correlations between biological activities and molecular descriptors for different classes of compounds (Bertoša et al., 2003; Ćaleta et al., 2009). In classical CoMFA (Comparative Molecular Field Analysis) procedure, Molecular Interaction Fields (MIFs) are used as the 3D descriptors (Kubinyi, 1993). The main disadvantage of such procedure is handling a large 3D descriptors that, beside useful information, contain also plenty of information that can be characterized as "noise". VolSurf program enables extraction of the information from MIFs into a few numerical descriptors which have clear physical or chemical meaning (Cruciani et al., 2000a,b). Such procedure does not depend on the alignment of the molecules. Number and kind of the produced descriptors depends on the choice of the probes used to generate MIFs. Beside structural properties of the molecule, VolSurf descriptors describe also its ADME (Absorption, Distribution, Metabolism, Excretion) properties. Using Partial Least Square (PLS) analysis, VolSurf descriptors can be correlated with measured activities in order to generate QSAR model.

In the presented work, we have built QSAR models on the serious of heterocyclic amides and quinolones with measured antitumor activity using the VolSurf+ program. The goals of the QSAR analysis were: (i) to produce trustful, robust and reliable models that can be used in planning future experiments and (ii) to find out which chemical and physical descriptors are the most relevant for inhibition of the tumor cell lines growth.

2. Methods

2.1. Dataset

The dataset used for building and validating QSAR models consists of 59 compounds whose antitumor activity was measured and described in the literature (Dogan Koružnjak et al., 2002; Jarak et al., 2005, 2006; Ester et al., 2009; Table S1 in supporting material). Based on the literature sources from three groups of authors, compounds can be divided in three groups (Scheme 1, Table S1 in supporting material). Their antitumor activities against seven cancer cell types (HeLa (cervical carcinoma), Hep-2 (laryngeal carcinoma), MCF-7 (breast carcinoma), SW 620 (colon carcinoma), MiaPaCa-2 (pancreatic carcinoma), H 460 (lung carcinoma), and WI 38 (diploid fibroblasts)) were tested in the same laboratory (Dogan Koružnjak et al., 2002; Jarak et al., 2005, 2006; Ester et al., 2009). Preliminary calculations showed that the best models were obtained when antitumor activity against MiaPaCa-2 and MCF-7 tumor cells was correlated with structural features of the compounds. Logarithmic values of IC_{50} (the micromolar concentration that causes a 50% reduction of the cell growth) against MiaPaCa-2 and MCF-7 cells were used as biological activities of the compounds in deriving QSAR models. For the inactive compounds whose IC_{50} values are not explicitly given in the literature, but just estimated as ">100", $\log IC_{50}$ was set to 2.70.

2.2. Calculation of molecular descriptors

Smile codes were used as inputs and the 3D structures of the compounds were generated by VolSurf+ program (Cruciani et al., 2000a,b). Considering high rigidity of the dataset compounds, VolSurf+ 3D structure generator was considered to be powerful enough to produce the most relevant conformers and no additional conformational search was applied. The GRID program (Goodford, 1985) was used to calculate Molecular Interaction Fields (MIFs) for the 3D structure of each compound. MIF is the 3D matrix generated by calculating noncovalent interactions between the target molecule situated in the center of the grid and the probes placed in the grid points. Grid spacing was set to 0.5 Å. Following probes were used: H_2O (the water molecule), O (sp^2 carbonyl oxygen atom), N1 (neutral NH group (e.g. amide)) and DRY (the hydrophobic probe). From the MIFs, VolSurf+ derived series of 128 descriptors that refer to molecular size and shape, to hydrophilic and hydrophobic regions and to the balance between them, to the "charge state" descriptors, to lipophilicity, to molecular diffusion, $\log P$, $\log D$, to the presence/distribution of pharmacophoric descriptors and to descriptors on some other relevant ADME properties. The definition of all 128 VolSurf+ descriptors is given in the VolSurf+ manual (Cruciani et al., 2000a,b).

2.3. Building and validation of QSAR models

The relationship between the structure based molecular descriptors and biological activity of the dataset compounds was determined using the Partial Least Square (PLS) analysis. The number of significant latent variables (nLV) and quality of the models were determined using the leave-one-out (LOO) cross-validation procedure. Standard deviation of error of calculation (SDEC) and standard deviation of error of prediction (SDEP) were calculated for each model. In order to make more realistic validation of the predictive power of the models, external validation was also performed. For that purpose, dataset compounds were divided into training set (used to built the model) and test set (used for external prediction). Distribution of the compounds in these two sets was made, either according to the literature source of the measured biological activity, or randomly. In both cases test set consisted of approximately 1/4 to 1/3 of the dataset compounds and training set of the rest. The SDEP for external validation was calculated using homemade program since this feature is no longer available in VolSurf+ program. In order to identify the descriptors with the highest (positive or negative) impact on biological activity of the compounds, products between PLS coefficient and average value of the descriptor were observed.

2.4. PCA based QSAR models

Principal Component Analysis (PCA) was performed on the descriptors of complete dataset compounds. PCA loadings were used for identifying the descriptors with the highest contribution to the first three principal components. PCA scores were used for

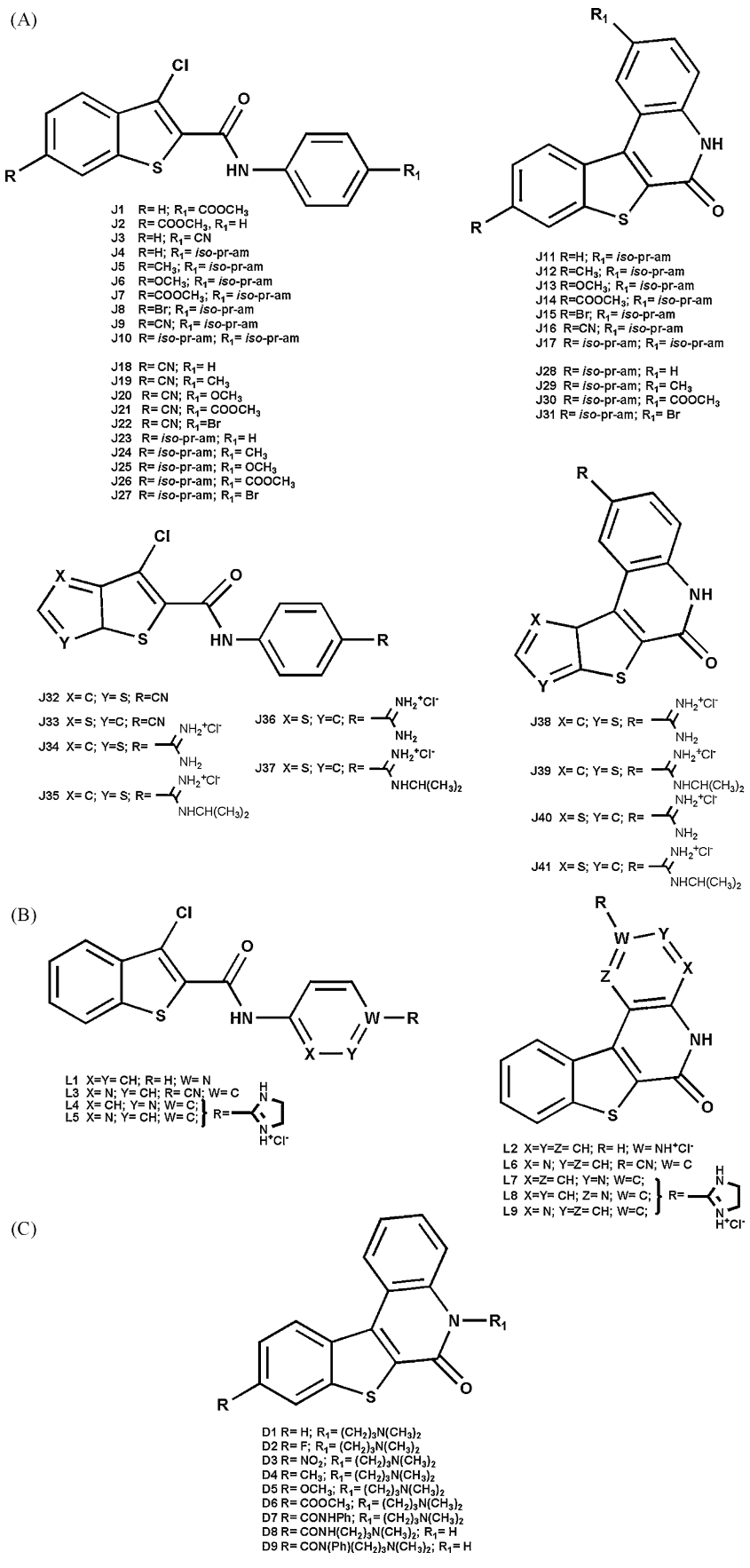

Scheme 1. Structures of the compounds used for building and validation of QSAR models. (A) Compounds J1–J41, (B) compounds L1–L9, (C) compounds D1–D9.

Table 1
Statistical properties of the QSAR models.

Model	nO[a]	nLV[b]	R^2	SDEC	Q^2	SDEP	SDEP-ext[c]	nOE[d]
1A	41	4	0.81	0.35	0.73	0.42	0.80	18
1B	41	4	0.72	0.47	0.59	0.56	0.60	18
2A	50	4	0.73	0.45	0.62	0.53	0.35	9
2B	50	4	0.69	0.49	0.54	0.59	0.71	9
3A	59 (56)[e]	3 (3)[e]	0.71 (0.77)[e]	0.47 (0.41)[e]	0.63 (0.70)[e]	0.53 (0.47)[e]	–	–
3B	59 (56)[f]	3 (3)[f]	0.65 (0.77)[f]	0.51 (0.41)[f]	0.56 (0.70)[f]	0.57 (0.46)[f]	–	–
4A	42	3	0.82	0.39	0.73	0.47	0.44	14
4B	43	3	0.78	0.42	0.68	0.50	0.15	13
5A	10	5	0.99	0.07	0.92	0.25	0.71	49
5B	10	5	0.99	0.07	0.92	0.21	0.62	49

[a] Number of objects used to built the model (training set).
[b] Number of latent variables.
[c] SDEP for the external prediction.
[d] Number of objects used for external prediction (test set).
[e] Calculated for the model in which three outliers have been expelled (L3, L7, L8, Table S1 in supporting material).
[f] Calculated for the model in which three outliers have been expelled (J6, J20, L3, Table S1 in supporting material).

deriving the small QSAR model. Based on the PCA scores for the first and the second principal component, compounds were clustered in 10 clusters. One compound from each cluster was chosen and the QSAR model was derived using only these 10 compounds (Fig. 4). Similar approach was already used in the study of specificity of binding of Ras proteins to their effectors (Tomić et al., 2007). Such model was tested for the prediction of biological activity of the rest 46 compounds.

3. Results and discussion

3.1. QSAR models 1A and 1B

QSAR model 1A and model 1B were built using 41 compounds (J1–J41 Table S1 in supporting material) whose biological activities were published in Jarak et al. (2005) and Jarak et al. (2006), and were tested on the remaining 18 dataset compounds (Dogan Koružnjak et al., 2003; Ester et al., 2009) (D1–D9 and L1–L9 Table S1 in supporting material).

Model 1A was build for their antitumor activity on MiaPaCa-2 (pancreatic carcinoma) cells. The best predictive ability of the model 1A (R^2 = 0.81, Q^2 = 0.73, SDEC = 0.35, SDEP = 0.42, Table 1) was found using 4 latent variables. Robustness of the model 1A was tested by external prediction. Despite high R^2 and Q^2 values, model 1A did not show good predictive ability towards the test set (SEDP = 0.80, Table 1, Fig. 1A). Such result can be explained with the fact that, in general, the compounds used to built the model 1A (Jarak et al., 2005, 2006) have weaker biological activities against MiaPaCa-2 cells (average log IC_{50} = 1.31) than the compounds that were used as the test set (average log IC_{50} = 0.30) (Dogan Koružnjak et al., 2003; Ester et al., 2009).

Model 1B was built in respect to antitumor activity towards MCF-7 (breast carcinoma) cells. The quality of the model 1B, according to the internal validation, was worse that the quality of model 1A (Table 1). On the other hand, its external prediction (SDEP = 0.60, Table 1, Fig. 1B) was better than in case of model 1A. The later is related to the fact that the experimental values of antitumor activity towards MCF-7 cells of the test set compounds (average log IC_{50} = 0.81) are more similar to the experimental values of the training set compounds (average log IC_{50} = 1.27) than it was the case for activities against MiaPaCa-2 cells.

3.2. QSAR models 2A and 2B

In order to increase the robustness, another two QSAR models, model 2A and model 2B, were derived for the 50 compounds from the three literal sources (Jarak et al., 2005, 2006; Ester et al.,

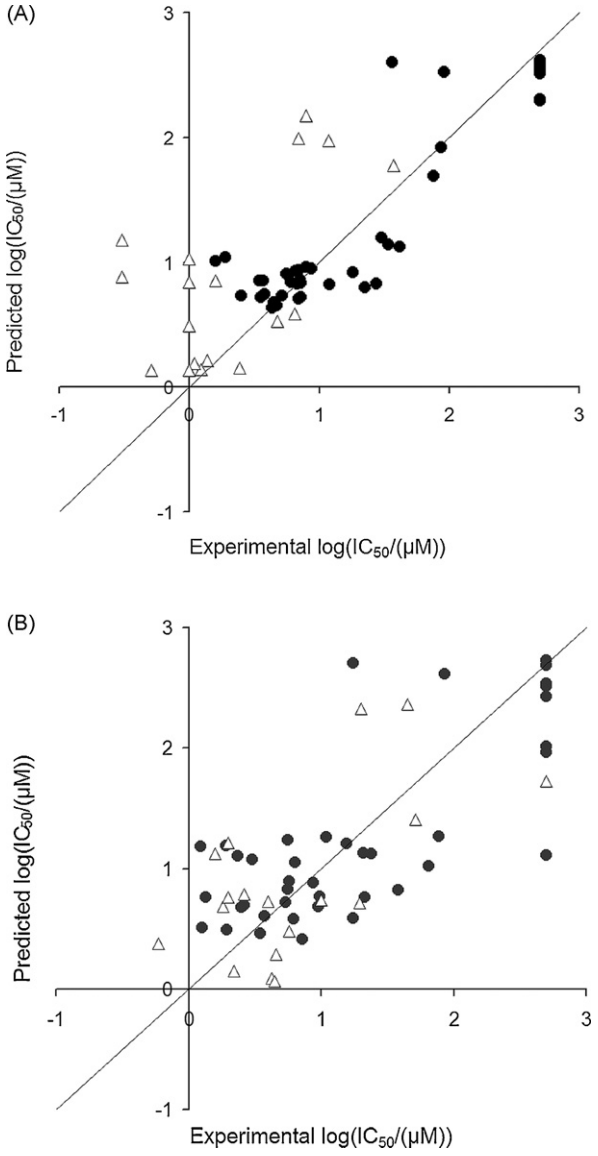

Fig. 1. Predicted vs experimental antitumor activity of: (A) model 1A, (B) model 1B. Black dots present training set compounds, white triangles present test set compounds.

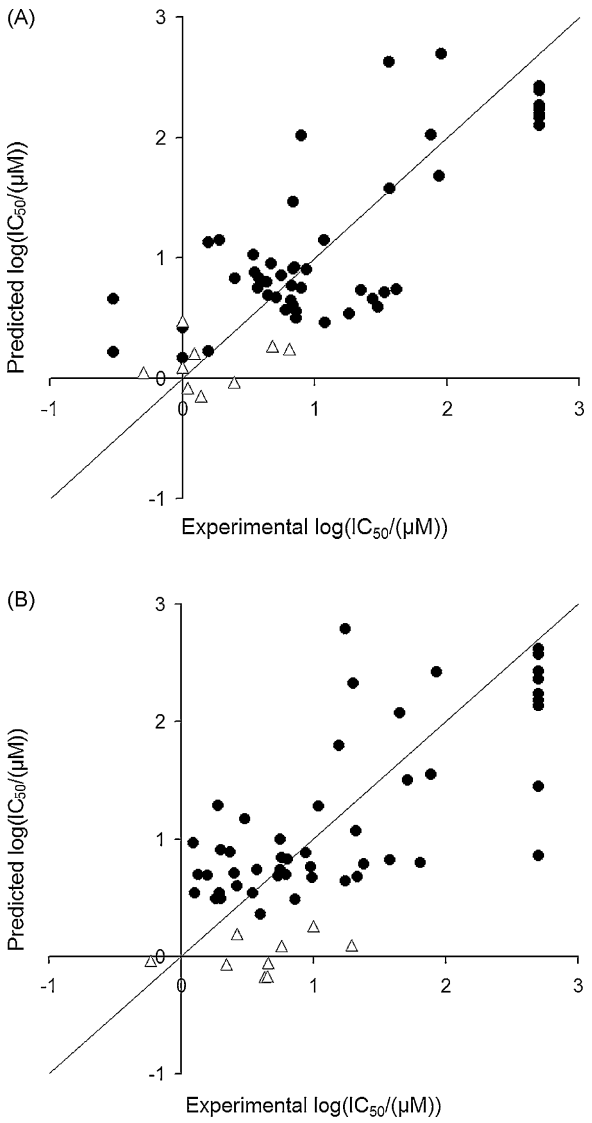

Fig. 2. Predicted vs experimental antitumor activity of: (A) model 2A, (B) model 2B. Black dots present training set compounds, white triangles present test set compounds.

2009) (J1–J41 and L1–L9, Table S1 in supporting material). The compounds from the fourth literal source (Dogan Koružnjak et al., 2003) (D1-D9, Table S1 in supporting material) served as the test set.

Model 2A was built using biological activity of the compounds towards MiaPaCa-2 (pancreatic carcinoma) cells. In respect to model 1A, quality of the model 2A decreased regarding internal validation (R^2 = 0.73, Q^2 = 0.62, SDEC = 0.45, SDEP = 0.53) (Table 1). However, the external prediction increased (SDEP = 0.35, Fig. 2A).

In the case of model 2B (built using antitumor activity towards MCF-7 (breast carcinoma) cells), both internal and external predictive performances decreased (Table 1, Fig. 2B).

3.3. QSAR models 3A and 3B

Model 3A and model 3B were built using data from all literal sources (Dogan Koružnjak et al., 2003; Jarak et al., 2005, 2006; Ester et al., 2009), 59 compounds in total (Table S1 in supporting material).

Model 3A was made using antitumor activity towards MiaPaCa-2 (pancreatic carcinoma) cells. Its internal validation (R^2 = 0.71, Q^2 = 0.63, SDEC = 0.47, SDEP = 0.53) was spoilt with three obvious outliers (L7, L8, L3 Table S1 in supporting material, Fig. S1 in supporting material). Exclusion of the outliers highly improved quality of the model (R^2 = 0.77, Q^2 = 0.70, SDEC = 0.41, SDEP = 0.47, Table 1).

Model 3B, built using biological activity towards MCF-7 (breast carcinoma) cells, showed similar behavior as model 3A. Exclusion of the three outliers (J6, J20, L3 Table S1 and Fig. S1 in supporting material) significantly improved quality of the model (R^2 = 0.77, Q^2 = 0.70, SDEC = 0.41, SDEP = 0.46, Table 1).

The robustness of the models 3A and 3B was not tested on the external prediction since all the dataset compounds were used as the training set. In order to enable testing of predictive ability towards external prediction, compounds were randomly divided in test set (approximately 1/4 of the dataset compounds, J4, J10, J13, J20, J27, J30, J32, J37, J39, J41, L1, L5, D6, D8) and training set (the rest of the dataset compounds). The compounds previously identified as outliers were excluded. In such way, model 4A and model 4B were built on the training set (using activity against MiaPaCa-2 and MCF-7 cells, respectively) and then tested for external prediction on the test set. Both models showed good quality regarding internal validation (model 4A – R^2 = 0.82, Q^2 = 0.73, SDEC = 0.39, SDEP = 0.47; model 4B – R^2 = 0.78, Q^2 = 0.68, SDEC = 0.42, SDEP = 0.50; Table 1),

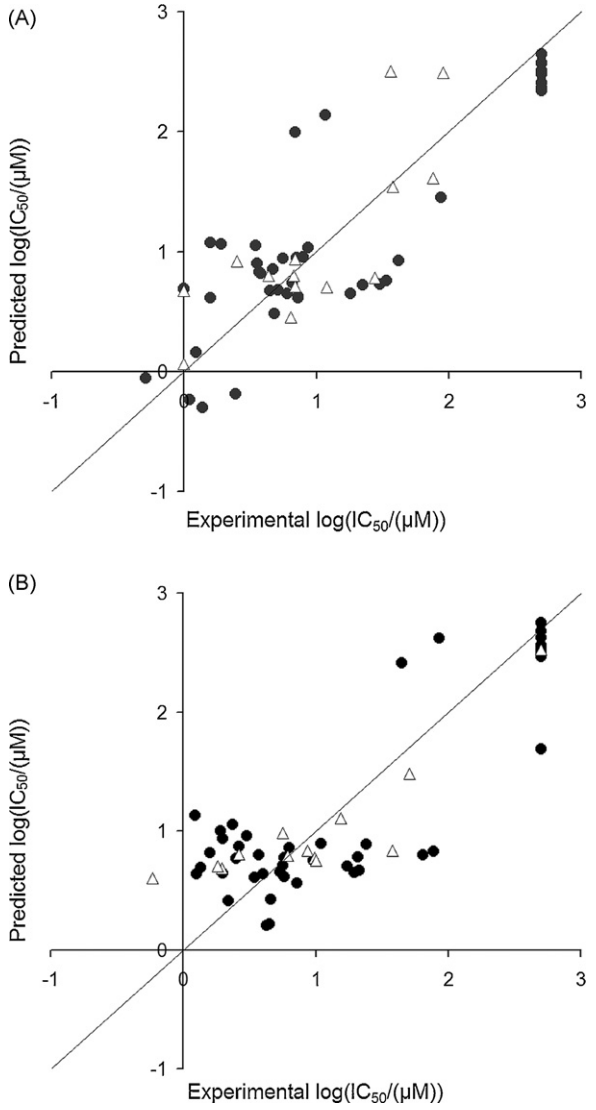

Fig. 3. Predicted vs experimental antitumor activity of: (A) model 4A, (B) model 4B. Black dots present training set compounds, white triangles present test set compounds.

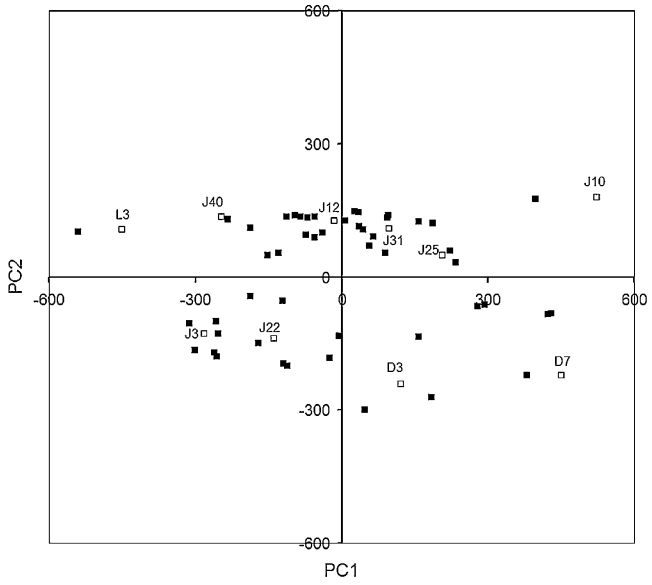

Fig. 4. PCA scores, 10 compounds chosen to built models 5A and 5B (PCA based QSAR models) are shown as white squares.

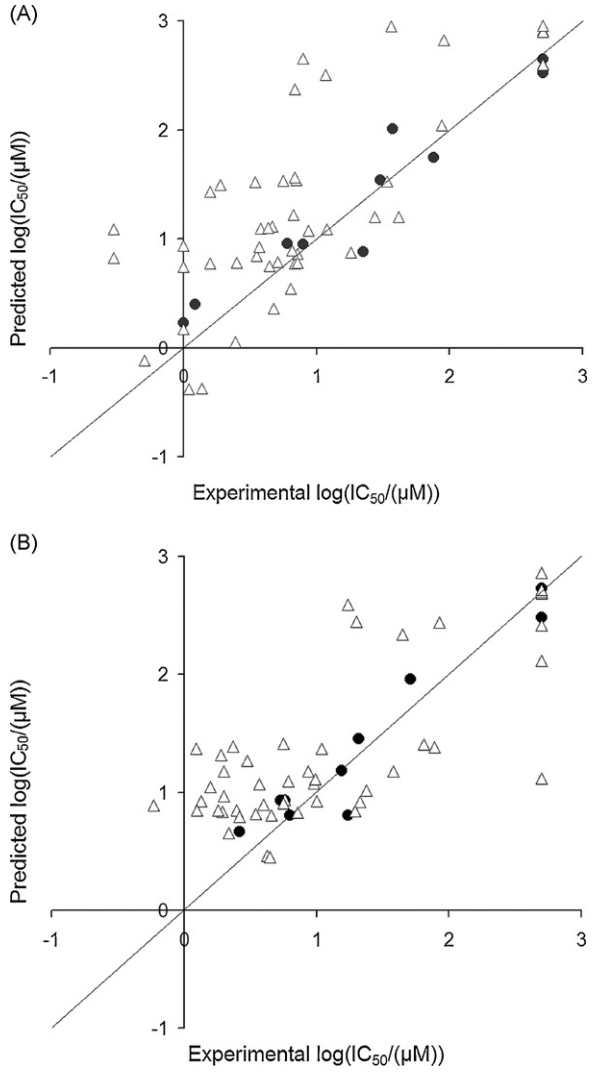

Fig. 5. Predicted vs experimental antitumor activity of: (A) model 5A, (B) model 5B. Black dots present training set compounds, white triangles present test set compounds.

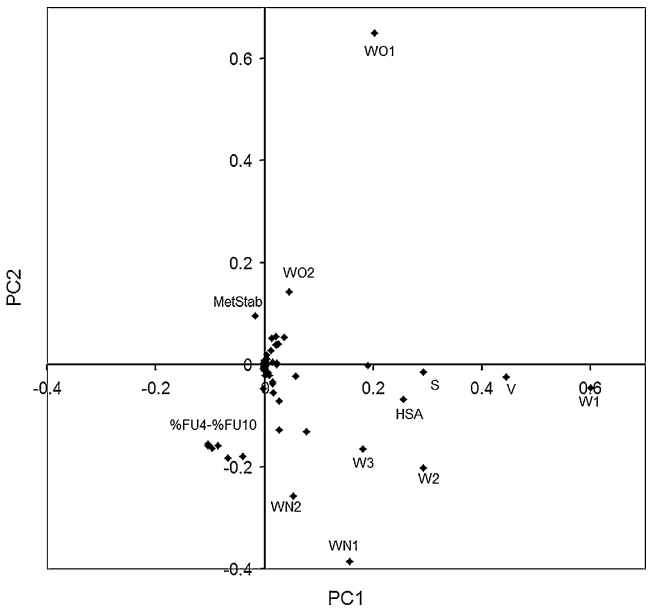

Fig. 6. Loadings for the first two principal components. PCA was performed on the overall dataset consisting of 59 compounds.

as well as regarding external prediction (model 4A: SDEP = 0.44, model 4B: SDEP = 0.15; Table 1, Fig. 3). Apparently both models are quite robust and should be helpful in choosing new candidates for synthesis.

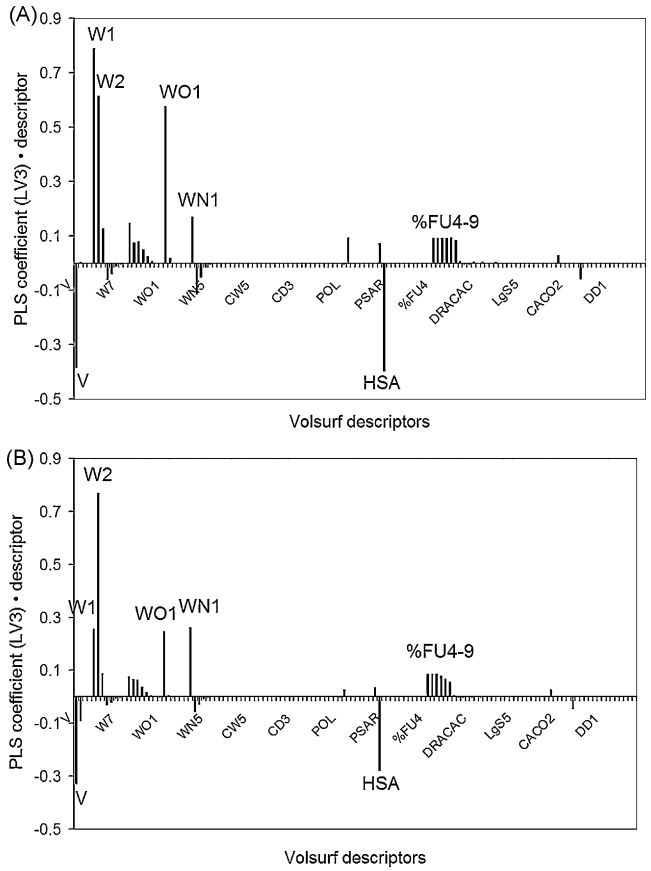

Fig. 7. Products of the descriptor's average value (calculated for the dataset used to built the model) and the associated PLS coefficient in case of: (A) model 4A, (B) model 4B. Descriptors with the highest impact on the activity are labeled; list and description of all 128 VolSurf+ descriptors is given in the VolSurf+ manual (Cruciani et al., 2000a,b).

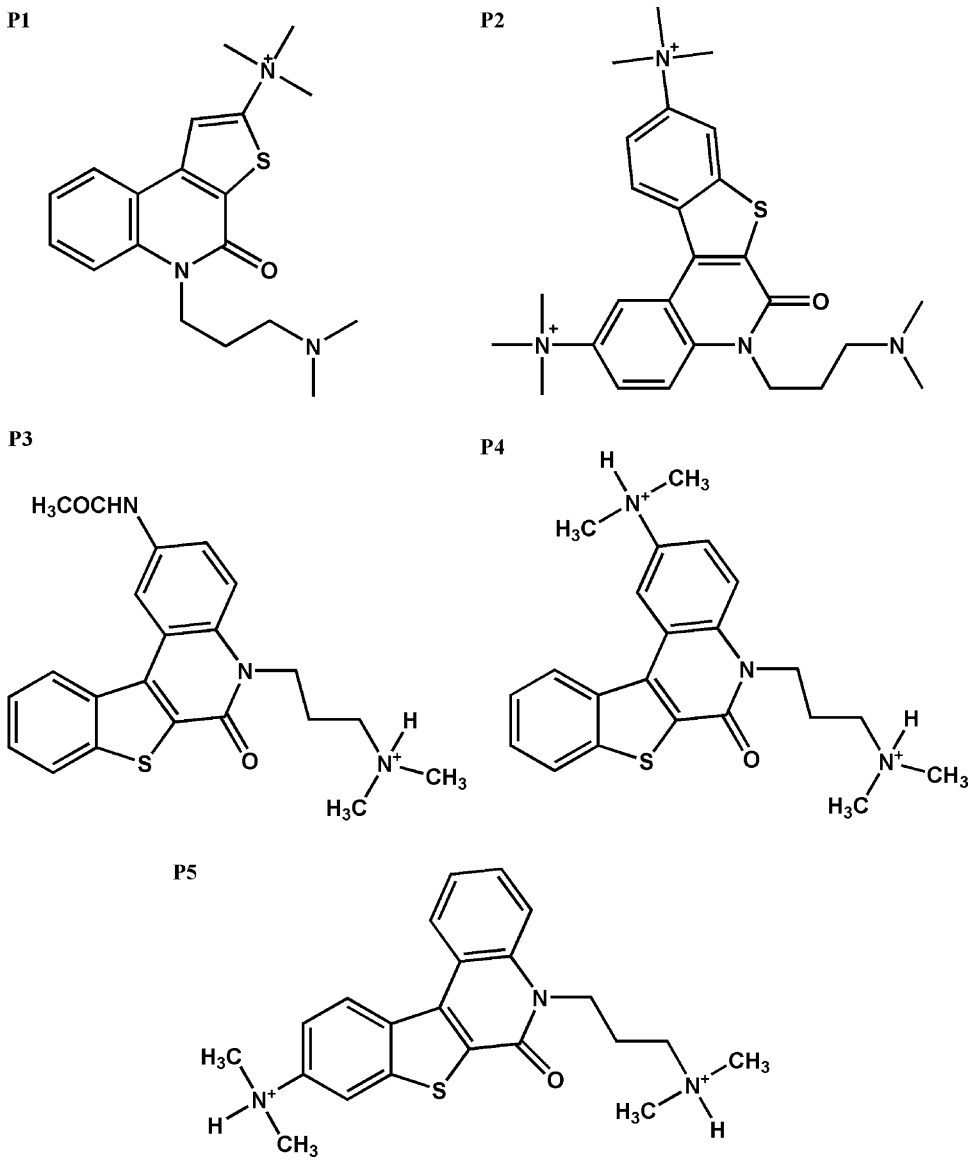

Fig. 8. Proposed molecules which should have pronounced antitumor activity against MiaPaCa-2 and MCF-7 cells.

3.4. PCA based QSAR models

Principal Component Analysis (PCA) was performed on the overall dataset (59 compounds). The first two principal components explained 73.4% of variance (the first three PCs explained 90.1%). Based on distribution of the compounds in the space of principal component (Fig. 4), 10 compounds (compounds: J3, L1, D3, D7, J10, J31, J12, J25, J22, J40, Table S1 in supporting material), were chosen to build the models. Model 5A was built using antitumor activity on MiaPaCa-2 (pancreatic carcinoma) cells. Model 5B was built using antitumor activity on MCF-7 (breast carcinoma) cells. External prediction of both models was tested on the rest of 49 compounds. The activities of the most of the test set compounds were predicted fairly well (Table 1, Fig. 5). Compounds with the highest error in prediction were previously mentioned outliers.

This result shows another possible application of computational approach in order to make experimental approach more efficient and faster. Instead of synthesizing all 59 compounds and measuring their biological activities in search for the most active ones, it would be faster and more efficient to built *in silico* all the compounds, perform principal component analysis and, according to the result, choose just a few of them (in our case 10) for synthesis and biological testing. The QSAR model derived on the selected compounds can be used to predict the activity of the rest of the compounds. That would enable the experimentalist to choose only the best candidates for future synthesis and biological measurements.

3.5. Molecular descriptors with the highest impact on the antitumor activity of quinolones

PCA loadings plot (Fig. 6) shows contribution of each descriptor to the first two principal components (PCs). Since PCs are constructed in a way that the first few components describe majority of the X-matrix variance, their loadings describe descriptors with the highest contribution to the overall variance in the X-space PCs (which implies that their variation between the compounds is the most pronounced). PCA on the complete dataset identified following descriptors as the ones with the highest variation between the compounds: WO1 (H-bond donor descriptor, calculated with carbonyl oxygen as the probe), WN1–WN4 (H-bond acceptor descriptor, calculated with neutral amide group as the

probe), W1–W4 (hydrophilic regions), *V* (volume), D1 (hydrophobic regions), *S* (surface), HSA (the sum of hydrophobic surface areas), %FU4–%FU9 (the percentage of unionized species calculated at pH 4, 5, 6, 7, 8 and 9).

The influence of each descriptor to the QSAR model can be estimated from its PLS coefficient, while the real impact of a descriptor on the biological activity is given as the product of the descriptor value and its PLS coefficient. If the product is positive, the descriptor negatively impacts the activity (it decreases activity), and another way around (*i.e.* smaller $\log IC_{50}$ means compound with higher activity). In order to investigate impact of each descriptor on the biological activity, product between average value of the descriptor (calculated for the dataset used to built the model) and its associated PLS coefficient was calculated for the models 4A and 4B (Fig. 7). Similar approach for identifying the most important descriptors has been used in investigation of *P*-glycoprotein interacting drugs (Zhuang et al., 2006). From the coefficients plot, Zhuang et al. concluded that size and shape descriptors, as well as descriptors of polarizability and descriptors related to compound's ability to make hydrogen bonds have marked influence on *P*-glycoprotein ATPase activity.

Apparently, descriptors with the highest positive impact on the measured anticancer activity (MiaPaCa-2 and MCF-7cells) are *V* (the water solvent excluded volume) and HSA (sum of hydrophobic surface areas). The later implies that increase in compound's volume and amount of hydrophobic surface areas (in respect to the volume and hydrophobic surface areas of the dataset compounds) should lead to increase in the biological activity. Descriptors with the highest negative impact on the biological activity are: W1–W2 (hydrophilic volumes calculated at energy levels from −0.2 to −0.5 kcal/mol, describing polarizability and dispersion forces), WO1 (H-bond donor regions at −1 kcal/mol energy level), WN1 (H-bond acceptor regions at energy level of −1 kcal/mol) and %FU4–%FU9 (the percentage of unionized species). The later finding is in accordance with recently published work of Madonna et al. (2010) in which they identified presence of a protonalbe function as one of the major structural conditions for antitumor activity of 8-hydroxyquinoline substituted benzylamines. It is interesting to notice that W4–W8 (hydrophilic volumes calculated at energy levels from −0.2 to −1.0 kcal/mol, describing polar and strong H-bond donor–acceptor regions) and WN2–WN6 (H-bond acceptor regions at energy levels from −2 to −6 kcal/mol) have small positive impact on biological activity.

Table 2
Predicted antitumor activity of the proposed compounds towards MiaPaCa-2 (models 1A–5A) and MCF-7 (models 1B–5B) cell lines.

QSAR models	$\log IC_{50}$ (μmol)				
	P1	P2	P3	P4	P5
1A	−0.20	−0.41	0.91	1.05	1.06
2A	−0.67	−0.30	0.82	0.83	0.93
3A	−0.46	−0.26	0.67	0.58	0.66
(3A)[a]	−0.34	−0.28	0.71	0.63	0.69
4A	−0.51	−0.44	0.66	0.60	0.66
5A	−0.31	−0.29	0.70	0.49	0.57
1B	−0.62	−0.79	1.23	1.00	1.01
2B	−0.62	−0.55	0.71	0.70	0.74
3B	0.02	−0.03	0.81	0.63	0.67
(3B)[b]	0.05	0.03	0.78	0.65	0.69
4B	0.06	0.06	0.79	0.59	0.64
5B	0.49	0.48	0.95	0.72	0.76

[a] Calculated for the model in which three outliers have been expelled (L3, L7, L8, Table S1 in supporting material).
[b] Calculated for the model in which three outliers have been expelled (J6, J20, L3, Table S1 in supporting material).

3.6. Proposal of the new compounds

Based on the QSAR analysis, new compounds are proposed (Fig. 8) whose biological activity should be higher comparing to the activity of dataset compounds. Proposed compounds (P1–P5) were derived from the compound D5 (Table S1 in supporting material) which has one of the largest antitumor activity against MiaPaCa-2 ($\log IC_{50} = -0.29$) and against MCF-7 ($\log IC_{50} = 0.34$) cells (Dogan Koružnjak et al., 2003). Proposed compounds were predicted by all models as active against both considered cell lines, MiaPaCa-2 and MCF-7 (Table 2). VolSurf+ software has already been used for predicting antitumor activity of novel heterocyclic compounds and experiments proved its reliability (Fortuna et al., 2008).

4. Conclusion

Models derived on the whole dataset were shown to be robust and can be used for predicting the activity of novel compounds. The model obtained for a small dataset selected according to the PCA scores can serve as a guideline for synthesis of new compounds. Apparently such approach can be useful in planning future experiments. The properties of the studied compounds which are the most important for their antitumor activity (MiaPaCa-2 and MCF-7 cells lies) were identified. We found that the presence of the group(s) that can be easily ionized in the pH range from 4 to 9 and the increase in the volume and in the amount of hydrophobic surfaces (in comparison to the dataset compounds), should lead to increase of antitumor activity against breast (MiaPaCa-2) and pancreatic (MCF-7) carcinoma. In the same time, polarizability, tendency to make dispersion forces and capability of a compound to be involved as the H-bond donor in the weak H-bond were found to have negative effect on the compound's antitumor activity against MiaPaCa-2 and MCF-7 cells. New compounds, which were predicted by derived QSAR models as promising antitumor agents against MiaPaCa-2 and MCF-7 cells, were proposed. The results of the presented work should be useful for synthesis of the new antitumor compounds against MiaPaCa-2 and MCF-7 tumor cells.

Acknowledgment

We gratefully acknowledge support by the Ministry of Science, Education and Sport of the Republic of Croatia (project 098-1191344-2860).

Appendix A. Supplementary data

Supplementary data associated with this article can be found, in the online version, at doi:10.1016/j.ijpharm.2010.05.014.

References

Bertoša, B., Kojić-Prodić, B., Ramek, M., Piperaki, S., Tsantili-Kakoulidou, A., Wade, R., Tomić, S., 2003. A new approach to predict the biological activity of molecules based on similarity of their interaction fields and the log *P* and log *D* values: application to auxins. J. Chem. Inform. Comput. Sci. (New Name: J. Chem. Inform. Model.) 43, 1532–1541.

Chen, Y.-L., Chung, C.-H., Chen, I.-L., Chen, P.-H., Jeng, H.-Y., 2002. Synthesis and cytotoxic activity evaluation of indolo-, pyrrolo-, and benzofuro-quinolin-2(1*H*)-ones and 6-anilinoindoloquinoline derivatives. Bioorg. Med. Chem. 10, 2705–2712.

Chilin, A., Marzano, C., Baccichetti, F., Simonato, M., Guiotto, A., 2000. 4-Hydroxymethyl- and 4-methoxymethylfuro[2,3-*h*]quinolin-2(1*H*)-ones: synthesis and biological properties. Bioorg. Med. Chem. 11, 1311–1318.

Coughlin, S.A., Danz, D.W., Robinson, R.G., Klingbeil, K.M., Wentland, M.P., Corbett, T.H., Waud, W.R., Zwelling, L.A., Altschuler, E., Bales, E., Rake, J.B., 1995. Mechanism of action and antitumor activity of (S)-10-(2,6-dimethyl-4-pyridynil)-9-fluoro-3-methyl-7-oxo-2,3-dihydro-7H-pyridol[1,2,3-DE]-[1,4]benzothiazine-6 carboxylic acid (WIN 58161). Biochem. Pharmacol. 50, 111–122.

Cruciani, G., Crivori, P., Carrupt, P.-A., Testa, B., 2000a. Molecular fields in quantitative structure–permeation relationships: the VolSurf approach. J. Mol. Struct.: THEOCHEM 503, 17–30.

Cruciani, G., Pastor, M., Guba, W., 2000b. VolSurf: a new tool for pharmacokinetic optimization of lead compounds. Eur. J. Pharm. Sci. 11, S29–S39.

Ćaleta, I., Kralj, M., Marjanović, M., Bertoša, B., Tomić, S., Pavlović, G., Pavelić, K., Karminski-Zamola, G., 2009. Novel cyano- and amidino-benzothiazole derivatives: synthesis, antitumor evaluation, X-ray and QSAR analysis. J. Med. Chem. 52, 1744–1756.

Dogan Koružnjak, J., Grdiša, M., Slade, N., Zamola, B., Pavelić, K., Karminski-Zamola, G., 2003. Novel derivatives of benzo[*b*]thieno[2,3-*c*]quinolones: synthesis, photochemical synthesis, and antitumor evaluation. J. Med. Chem. 46, 4516–4524.

Dogan Koružnjak, J., Slade, N., Zamola, B., Pavelić, K., Karminski-Zamola, G., 2002. Synthesis, photochemical synthesis and antitumor evaluation of novel derivatives of thieno[3′,2′:4,5]thieno[2,3-*c*]quinolones. Chem. Pharm. Bull. 50, 656–660.

Ester, K., Hranjec, M., Piantanida, I., Ćaleta, I., Jarak, I., Pavelić, K., Kralj, M., Karminski-Zamola, G., 2009. Novel derivatives of pyridylbenzo[*b*]thiophene-2-carboxamides and benzo[*b*]thieno[2,3-*c*]naphthyridin-2-ones: minor structural variations provoke major differences of antitumor action mechanisms. J. Med. Chem. 52, 2482–3249.

Fortuna, C.G., Barresi, V., Berellini, G., Musumarra, G., 2008. Design and synthesis of trans 2-(furan-2-yl)vinylheteroaromatic iodides with antitumour activity. Bioorg. Med. Chem. 16, 4150–4159.

Goodford, P.J., 1985. Computational procedure for determining energetically favorable binding sites on biologically important macromolecules. J. Med. Chem. 28, 849–857.

Jarak, I., Kralj, M., Šuman, L., Pavlović, G., Dogan, J., Piantanida, I., Žinić, M., Pavelić, K., Karminski-Zamola, G., 2005. Novel cyano- and *N*-isopropylamidino-substituted derivatives of benzo[*b*]thiophene-2-carboxanilides and benzo[*b*]thieno[2,3-*c*]quinolones: synthesis, photochemical synthesis, crystal structure determination and antitumor evaluation. J. Med. Chem. 48, 2346–2360.

Jarak, I., Kralj, M., Piantanida, I., Šuman, L., Žinić, M., Pavelić, K., Karminski-Zamola, G., 2006. Novel cyano- and amidino-substituted derivatives of thieno[2,3-*b*]- and Thieno[3,2-*b*]thiophene-2-carboxanilides and thieno[3′,2′:4,5]thieno- and thieno[2′,3′:4,5]thieno[2,3-*c*]quinolones: synthesis, photochemical synthesis, DNA binding and antitumor evaluation. Bioorg. Med. Chem. 14, 2859–2868.

Kubinyi, H. (Ed.), 1993. 3D QSAR in Drug Design. Theory, Methods and Applications, ESCOM. Science Publishers B.V., Leiden.

Kwok, Y., Sun, D., Clement, J.J., Hurley, L.H., 1999. The quinobenzoxazines: relationship between DNA binding and biological activity. Anti-Cancer Drug Design 14, 443–450.

Marzano, C., Chilin, A., Baccichetti, F., Bettio, F., Guiotto, A., Miolo, G., Bordin, F., 2004. 1,4,8-Trimethylfuro[2,3-*H*]quinolin-2(1*H*)-one, a new furocoumarin bioisoster. Eur. J. Med. Chem. 39, 411–419.

Madonna, S., Beclin, C., Laras, Y., Moret, V., Marcowycz, A., Lamoral-Theys, D., Dubois, J., Barthelemy-Requin, M., Lenglet, G., Depauw, S., Cresteil, T., Aubert, G., Monnier, V., Kiss, R., David-Cordonnier, M.-H., Kraus, J.-L., 2010. Structure–activity relationships and mechanism of action of antitumor bis8-hydroxyquinoline substituted benzylamines. Eur. J. Med. Chem. 45, 623–638.

Tomić, S., Bertoša, B., Wang, T., Wade, R.C., 2007. COMBINE analysis of the specificity of binding of Ras proteins to their effectors. Proteins: Struct. Funct. Bioinform. 67, 435–447.

Xia, Y., Yang, Z.-Y., Hour, M.-J., Kuo, S.-C., Xia, P., Bastow, K.F., Nakanishi, Y., Nampoothiri, P., Hackl, T., Hamel, E., Lee, K.-H., 2001. Antitumor agents. Part 204:[1] synthesis and biological evaluation of substituted 2-aryl quinazolinones. Bioorg. Med. Chem. Lett. 11, 1193–1196.

Yang, Z.-Y., Xia, Y., Xia, P., Tachibana, Y., Bastow, K.F., Lee, K.-H., 1999. Antitumor agents 1871: synthesis and cytotoxicity of substituted 8,8-dimethyl-2H,8H-pyrano[6,5-*h*]quinoline-2-one and related compounds. Bioorg. Med. Chem. Lett. 9, 713–716.

Zhuang, X.-M., Xiao, J.-H., Li, J.-T., Zhang, Z.-Q., Ruan, J.-X., 2006. A simplified model to predict *P*-glycoprotein interacting drugs from 3D molecular interaction field. Int. J. Pharm. 309, 109–114.